# Kinetic Results and Reaction Pathways of Intermolecular Thiolato Ligand Migration between Titanocene Complexes and from $Cp_2TiX(SAr)$ (X = Cl, SAr) to PtCl(Me)(cod) (cod = $\eta^2,\eta^2$-1,5-Cyclooctadiene)

**Kohtaro Osakada,* Tomoya Hosoda, and Takakazu Yamamoto***

Research Laboratory of Resources Utilization, Tokyo Institute of Technology, 4259 Nagatsuta, Midori-ku, Yokohama 226-8503

(Received November 10, 1999)

$Cp_2TiCl(SPh)$ (**1a**), prepared from an equimolar reaction of $Cp_2TiCl_2$ with NaSPh, undergoes partial and reversible disproportionation in THF into $Cp_2TiCl_2$ and $Cp_2Ti(SPh)_2$ (**2a**). The thermodynamic parameters of the reaction are determined to be $\Delta H^\circ$ = 13.0(0.6) kJ mol$^{-1}$ and $\Delta S^\circ$ = 14(2) J K$^{-1}$ mol$^{-1}$ at 298 K. An equimolar reaction of $Cp_2Ti(SAr)_2$ (**2a**: Ar = $C_6H_5$, **2b**: Ar = $C_6H_4Me$-*p*, **2c**: Ar = $C_6H_4OMe$-*p*, **2d**: Ar = $C_6H_4Cl$-*p*, **2e**: Ar = $C_{10}H_7$) with PtCl(Me)(cod) in THF leads to an intermolecular exchange of the thiolato and chloro ligands to afford Pt(Me)(SAr)(cod) (**3a**: Ar = $C_6H_5$, **3b**: Ar = $C_6H_4Me$-*p*, **3c**: Ar = $C_6H_4OMe$-*p*, **3d**: Ar = $C_6H_4Cl$-*p*, **3e**: Ar = $C_{10}H_7$). Ti complexes: $Cp_2TiCl_2$, $Cp_2TiCl(SAr)$, $Cp_2Ti(SAr)_2$, and a minor amount of $(Cp_2TiCl)_2O$, are also present in the products. Absorption spectra of a solution of **2a** and excess PtCl(Me)(cod) exhibit distinct changes due to the thiolato ligand transfer, and indicate initial formation of **1a** and its subsequent reaction with the Pt complex to form $Cp_2TiCl_2$. The reaction of **1a** with excess PtCl(Me)(cod) obeys second-order kinetics to [**1a**]. The observed rate constants, $k_{obsd}$, increase with an increase in the concentration of PtCl(Me)(cod). Linear plots of the reciprocal of $k_{obsd}$ versus $[\mathbf{1a}]_0/[PtCl(Me)(cod)]_0$ are consistent with the reaction pathway involving the disproportionation of **1a** into an equimolar mixture of $Cp_2TiCl_2$ and **2a**, the latter of which readily reacts with PtCl(Me)(cod) to regenerate **1a**.

The reactions of bis(cyclopentadienyl)bis(thiolato)-titanium(IV) with chloro complexes of late transition metals were reported to cause intermolecular exchanges of these ligands.[1—5] The reactions form Ti–Cl and M–S bonds (M = Co, Ni, Pd, and Pt) accompanied by cleavage of Ti–S and M–Cl bonds of the starting complexes. Mismatching in coordination of soft thiolato ligand and hard Ti(IV) center is relieved when the reaction proceeds. This thermodynamic motivation brings about the high performance of the reaction under mild conditions. High selectivity of the reaction without use of basic NaSR or toxic $Tl(SR)_3$ allows the convenient synthesis of late transition metal complexes with thiolato ligands.

Previously we reported the thiolato ligand transfer from $Cp_2Ti(SR)_2$ (R = Et, *i*-Pr) and $Cp_2Ti(SPh)_2$ to $PtCl_2(cod)$ giving $[Pt(SR)_2]_n$ and $Pt(SPh)_2(cod)$, respectively; this transfer was investigated kinetically.[5] $Cp_2TiCl(SEt)$, generated in situ from the reaction of $Cp_2Ti(SEt)_2$ and $PtCl_2(cod)$, reacted with excess $PtCl_2(cod)$ to give $Cp_2TiCl_2$. Similar thiolato group transfer from bis(cyclopentadienyl)bis(thiolato)-titanium(IV) to PtCl(R)(L) type complexes would provide a new preparation method for the Pt complexes with both alkyl and thiolato ligands. Mechanistic studies on the reaction will also be of interest since the alkyl ligand influences the rate of thiolato ligand transfer as well as its reaction pathway. In this paper we report the reactions of PtCl(Me)(cod) with $Cp_2TiCl(SAr)$ (**1**) and with $Cp_2Ti(SAr)_2$ (**2**) leading to intermolecular exchange of the thiolato and chloro ligands to give PtMe(SAr)(cod). Kinetic results of the reaction with **1** have revealed a novel reaction pathway involving thiolato ligand migration among titanocene complexes prior to the chloro and thiolato ligand exchanges between Ti and Pt complexes. Structural and chemical properties of the Ti and Pt complexes relating to the mechanism of the thiolato ligand transfer from Ti to Pt complexes are also described.

## Results and Discussion

**Preparation, Structure, and Schlenk Type Equilibrium of $Cp_2TiCl(SPh)$ (1a).** An equimolar reaction of $Cp_2TiCl_2$ with NaSPh and purification of the products afforded $Cp_2TiCl(SPh)$ (**1a**) as deep red crystals. $Cp_2TiCl_2$, $Cp_2Ti(SPh)_2$ (**2a**), and other Ti-containing minor impurities in the reaction mixture were removed by careful recrystallization from $CH_2Cl_2$–$Et_2O$. Figure 1 depicts the results of an X-ray diffraction study. The molecular structure of **1a** is similar to that of other titanocene complexes with two anionic ligands and shows a Ti–S bond distance (2.389(5) Å) similar to those of **2a**.[7] As depicted in Fig. 2a, the $^1$H NMR spectrum of **1a** in THF-$d_8$ contains three signals at $\delta$ = 6.04, 6.26, and 6.55, which are assigned to hydrogens of the Cp ligands of **2a**, **1a**, and $Cp_2TiCl_2$, respectively. Signals of phenyl hydrogens of **2a** are also observed. Since the spectrum of **1a** obtained soon after dissolution of the complex shows the presence of these Ti complexes, **1a** undergoes rapid disproportionation

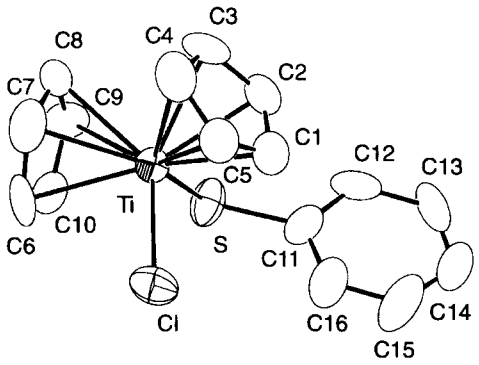


Fig. 1. ORTEP[6] drawing of $Cp_2TiCl(SPh)$ (**1a**) with 30% ellipsoidal levels. Cyclopentadienyl carbon atoms were refined isotropically. Selected bond distances (Å) and angles (°): Ti–Cl 2.378(6), Ti–S 2.389(5), S–C11 1.78(2), Ti–S–C11 114.4(7).

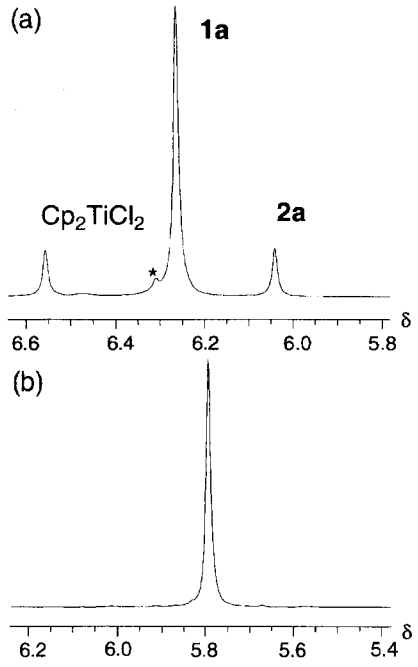


Fig. 2. $^1$H NMR spectra of **1a** in (a) THF-$d_8$ and (b) benzene-$d_6$ (cyclopentadienyl hydrogen region). A peak with an asterisk is due to uncharacterized impurity probably formed during the NMR sample preparation.

into an equimolar mixture of $Cp_2TiCl_2$ and **2a**, as shown in Eq. 1.

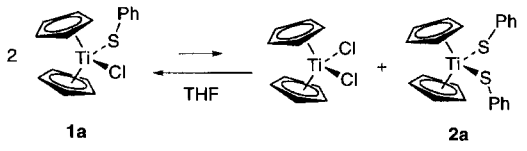


(1)

NMR spectra of the mixture taken at variant temperatures indicate reversible changes among these complexes in the temperature range of 300—323 K. The thermodynamic parameters of reaction (1) are determined to be $\Delta H^\circ = 13.0(0.6)$ kJ mol$^{-1}$ and $\Delta S^\circ = 14(2)$ J K$^{-1}$ mol$^{-1}$ at 298 K, based on the equilibrium constants obtained from the $^1$H NMR peak area ratios of the cyclopentadienyl hydrogens (Fig. 3). The peak intensity of **2a** and $Cp_2TiCl_2$ is much smaller than that of **1a**, suggesting that the equilibrium is favored for the formation of **1a**. The $^1$H NMR spectrum of **1a** in benzene-$d_6$ (Fig. 2b), however, showed a single resonance at $\delta = 5.79$ that can be assigned to the cyclopentadienyl hydrogens, when **1a** was left to stand for 10 min at room temperature prior to measurement. Leaving the solution further at room temperature led to generation of signals due to **2a** and $Cp_2TiCl_2$. Equilibrium was reached after about 2 h. The disproportionation of **1a** in benzene is much slower than that in THF.

Scheme 1 depicts two possible pathways for the disproportionation. Initial association of two $Cp_2TiCl(SPh)$ molecules by bridging chloro and thiolato ligands leads to intermolecular ligand transfer giving $Cp_2TiCl_2$ and $Cp_2Ti(SPh)_2$, as shown in Scheme 1(i). Association of $Cp_2Ti(SCH_2CH_2S)$ in the solid state and in solution was confirmed by X-ray crystallography and by the chemical properties of the complex.[5,8] An alternative pathway involves dissociation of a chloro ligand, followed by nucleophilic attack of a thiolato ligand of $Cp_2TiCl(SPh)$ on the cationic Ti complex (Scheme 1(ii)). The former pathway for the disproportionation seems to be more favorable, based on the kinetic results of the reaction of $Cp_2TiCl(SPh)$ with PtCl(Me)(cod) described later.

**Reactions of PtCl(Me)(cod) with $Cp_2Ti(SAr)_2$ (2) and $Cp_2TiCl(SAr)$ (1).** Equimolar reactions of PtCl(Me)(cod) with $Cp_2Ti(SAr)_2$ (**2a**: Ar = $C_6H_5$, **2b**: Ar = $C_6H_4Me$-*p*, **2c**: Ar = $C_6H_4OMe$-*p*, **2d**: Ar = $C_6H_4Cl$-*p*, **2e**: Ar = $C_{10}H_7$) proceeded smoothly in THF at room temperature to give methyl(arylthiolato)platinum complexes with a cod ligand, PtMe(SAr)(cod) (**3a**: Ar = $C_6H_5$, **3b**: Ar = $C_6H_4Me$-*p*, **3c**: Ar = $C_6H_4OMe$-*p*, **3d**: Ar = $C_6H_4Cl$-*p*, **3e**: Ar = $C_{10}H_7$) (Eq. 2). Table 1 summarizes the yields and analytical data of the complexes. Although some of the yields are moderate due to loss during isolation of the Pt complex from the mixture containing Ti complexes, conversion of PtCl(Me)(cod) into the thiolato complexes is almost quantitative. The reaction did not give any other Pt complexes, indicating that methyl ligand bonded to the Pt center did not participate in the intermolecular ligand transfer. The reaction of **2a** with PtCl-

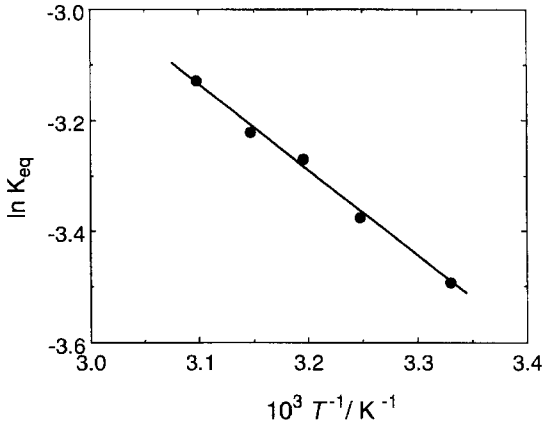


Fig. 3. Van't Hoff plots of the disproportionation shown in Eq. 1 in THF-$d_8$.

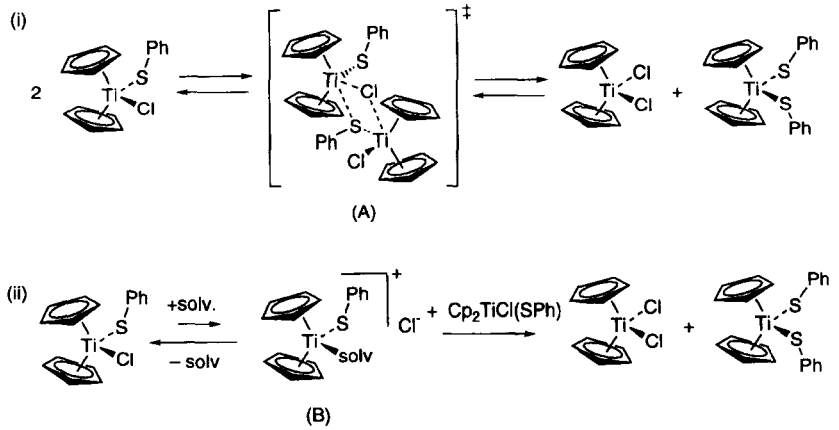


Scheme 1.

Table 1. Yields and Analytical Data of PtMe(SAr)(cod)

| Complex | Ar | Yield[a] | Analyses[b] | | |
|---|---|---|---|---|---|
| | | % | C (%) | H (%) | S (%) |
| **3a** | $C_6H_5$ | 75 | 42.30 (42.15) | 4.49 (4.70) | 7.40 (7.50) |
| **3b** | $C_6H_4Me$-*p* | 77 | 43.53 (43.52) | 4.83 (5.00) | 7.44 (7.25) |
| **3c** | $C_6H_4OMe$-*p* | 70 | 41.95 (42.00) | 4.84 (4.84) | 7.14 (7.00) |
| **3d** | $C_6H_4Cl$-*p* | 51 | 39.05 (39.00) | 3.88 (4.14) | 7.00 (6.94)[c] |
| **3e** | $C_{10}H_7$ | 55 | 47.48 (47.78) | 4.22 (4.64) | 6.57 (6.71) |

a) Isolated yield. b) Required values are given in parentheses. c) Cl: 7.66 (7.67).

(Me)(cod) in benzene did not occur under similar conditions.

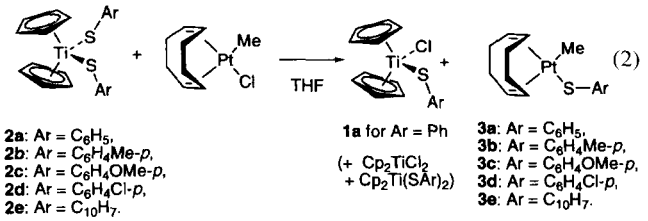


Figure 4 shows the molecular structure of **3a** with a square planar coordination around the Pt center. The Pt–S bond distance (2.287(3) Å) is within the range of already reported distances for thiolatoplatinum(II) complexes (2.276—2.374 Å).[9,10] Two double bonds of the cod ligand coordinate to the Pt center with significantly different Pt–C bond distances. Pt–C8 and Pt–C15 bond distances (2.276(10) and 2.252(9) Å) longer than the other Pt–C bond distances (Pt–C11 2.122(9) Å and Pt–C12 2.156(10) Å) suggest a larger trans influence of the methyl ligand compared with that of the phenylthiolato ligand. Complexes **3a**—**3e** give $^1$H NMR spectra which confirm the proposed structure, as summarized in Table 2. The vinyl hydrogen signals of the cod ligand and the methyl hydrogen signal are flanked by satellite signals. Larger $J$(PtH) values of the =CH– signal at $\delta$ = 3.99—4.54 ($J$ = 53—58 Hz) than that at $\delta$ = 4.78—4.92 ($J$ = 34—38 Hz) are ascribed to the difference in the degree of trans influence between the methyl and thiolato ligands which are situated at trans positions of the olefinic groups. The products contain $Cp_2TiCl_2$, $Cp_2TiCl(SAr)$, and $Cp_2Ti(SAr)_2$, which were identified by $^1$H NMR spectra. Although $Cp_2TiCl(SAr)$ (**1b**: Ar = $C_6H_4Me$-*p*, **1c**: Ar = $C_6H_4OMe$-*p*, **1d**: Ar = $C_6H_4Cl$-*p*, **1e**: Ar = $C_{10}H_7$) were not isolated, the $^1$H NMR signals in the reaction mixture were assigned well. The $^1$H NMR spectra often showed signals due to $[(Cp_2Ti)_2O]$ which is a secondary product of the reaction formed via hydrolysis of the thiolatotitanocene complexes by a trace amount of water contained in the solvent. The 1 : 2 reaction of **2a** and PtCl(Me)(cod) gave **3a** and $Cp_2TiCl_2$. Formation of $[(Cp_2Ti)_2O]$ was not observed.

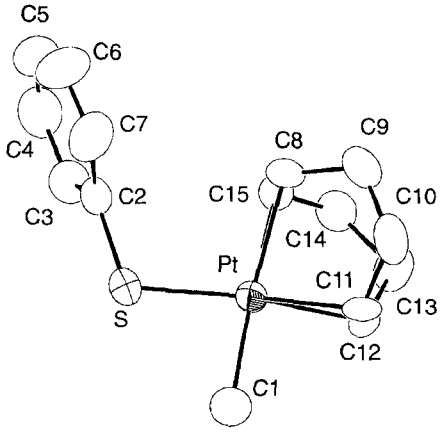


Fig. 4. ORTEP drawing of PtMe(SPh)(cod) (**3a**) with 30% ellipsoidal levels. Selected bond distances (Å) and angles (°): Pt–C1 2.05(1), Pt–C8 2.276(10), Pt–C11 2.122(9), Pt–C12 2.156(10), Pt–C15 2.252(9), C8–C15 1.38(1), C11–C12 1.41(1), Pt–S 2.287(3), S–C2 1.76(1), S–Pt–C1 83.5(3), Pt–S–C2 111.2(3).

**UV-vis Spectra Change in the Reaction of 2a with Excess PtCl(Me)(cod).** Addition of a THF solution of **2a**

Table 2. $^1$H NMR Data of PtMe(SAr)(cod)[a)]

| | $CH_3$ [b)] | $CH_2$ | CH= [b)] | CH= [b)] | Aromatic[c)] | | |
|---|---|---|---|---|---|---|---|
| | | | | | *meta* | *para* | *ortho* |
| **3a** | 0.99 (s) [75] | 1.33—1.83(m) | 3.99 (s) [55] | 4.89 (s) [37] | 6.94 (d, 7—8) | 7.09 (t, 8) | 7.79 (d, 7) |
| **3b**[d)] | 1.01 (s) [75] | 1.38—1.84(m) | 4.01 (s) [58] | 4.92 (s) [38] | 6.93 (d, 8) | | 7.72 (d, 8) |
| **3c**[e)] | 1.01 (s) [75] | 1.34—1.80(m) | 4.03 (s) [58] | 4.92 (s) [38] | 6.72 (d, 9) | | 7.69 (d, 9) |
| **3d** | 0.90 (s) [75] | 1.37—1.83(m) | 3.98 (s) [53] | 4.78 (s) [34] | 7.02 (d, 8) | | 7.48 (d, 8) |
| **3e** | 0.58 (s) [76] | 2.07—2.53(m) | 4.54 (s) [55] | 4.86 (br) | | 7.33—7.91 (m)[f)] | |

a) Obtained in benzene-$d_6$ (**3a**—**3d**) and in $CD_2Cl_2$ (**3e**) at room temperature (ca. 25 °C). b) $J$(PtH) are shown in brackets. c) $J$(HH) is shown in parentheses. d) $CH_3$ 2.11 (s). e) $OCH_3$ 3.26 (s). f) Assignment of the peaks was not feasible due to severe ovelapping of the signals.

to a large excess (> 10 equiv) of PtCl(Me)(cod) causes a color change of the solution from purple to red. Changes in the absorption spectra during the reaction are shown in Fig. 5a. The initial peaks at 540 and 398 nm, which are assigned respectively to the LMCT and $\pi$–$\pi^*$ transition of **2a** (peaks (i) and (ii)), decrease rapidly and almost disappear in approximately 30 min. New peaks are soon generated at similar positions (500 and 443 nm) to those of **1a** (peaks (iii) and (iv)). Further reaction leads to the gradual decrease in the amount of once formed **1a** and to the formation of $Cp_2TiCl_2$ that exhibits a characteristic peak at 385 nm (peak (v)). Scheme 2 depicts the reaction pathway to account for the above changes in the spectra.

Stepwise displacement of the two phenylthiolato ligands of **2a** with Cl ligands of two PtCl(Me)(cod) molecules occurs via the intermediate complex **1a** which is formed from the reaction of **2a** with PtCl(Me)(cod) and is converted upon the reaction with the Pt complex into $Cp_2TiCl_2$. The former step proceeds more rapidly than the latter, suggesting a higher reactivity of the Ti–S bonds in **2a** than those in **1a**. A thiolato ligand transfer reaction of $Cp_2Ti(SR)_2$ (R = Et, *i*-Pr) with $PtCl_2$(cod) took place more rapidly than that of $Cp_2TiCl(SR)$.[5]

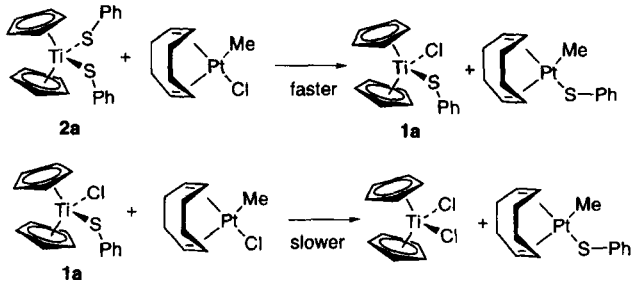


Scheme 2.

**Kinetics of the Reaction with 1a.** Figure 5(b) shows changes in the absorption spectra during the reaction of **1a**

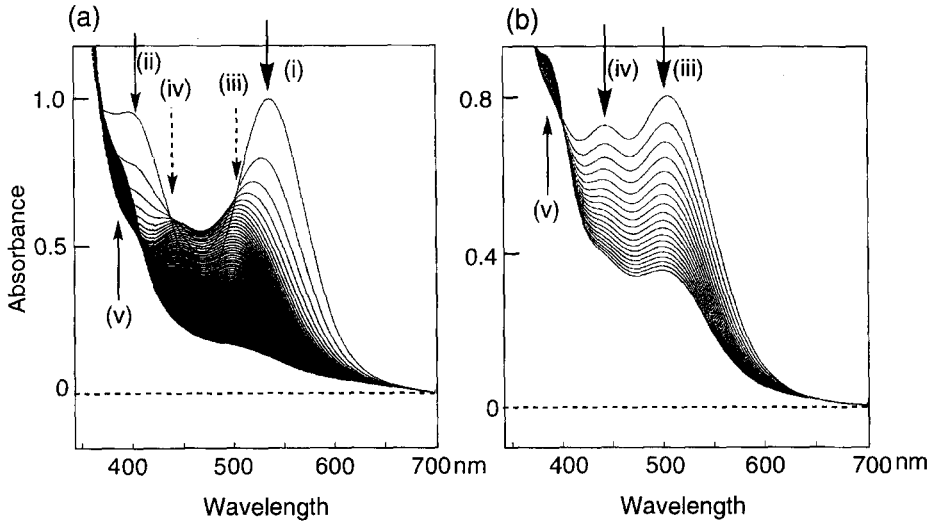


Fig. 5. (a) Change in the absorption spectra of a reaction mixture of **2a** (0.164 mM) and PtCl(Me)(cod) (10.9 mM) in THF at 25.5 °C. Spectra were recorded in every 10 min. Arrows in the spectra show the positions of the peak due to **2a** ((i) and (ii)), **1a** ((iii) and (iv)) and $Cp_2TiCl_2$ (v). (b) Change in the spectra of the reaction mixture of **1a** (0.31 mM) with PtCl(Me)(cod) (14.8 mM) at 31.5 °C. Spectra were recorded at every 10 min.

with excess PtCl(Me)(cod) in THF at somewhat higher temperature. A gradual decrease in the amount of **1a** and an increase in the intensity of a peak due to $Cp_2TiCl_2$ are observed with a clear isosbestic point at 406 nm. The spectroscopic change suggests the occurrence of the reaction shown in Eq. 3, although a detailed study of the reaction shown below has revealed a more complicated pathway for the reaction than the direct ligand exchange.

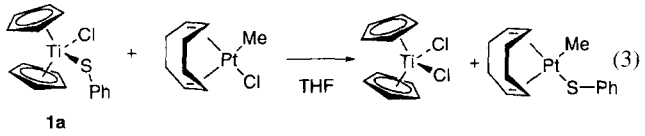


(3)

The reaction that is followed by decrease in intensity of the peak of **1a** at 500 nm obeys second-order kinetics to [**1a**],

$$-(\mathrm{d}[\mathbf{1a}]/\mathrm{d}t) = k_{\mathrm{obsd}}[\mathbf{1a}]^2, \quad (4)$$

rather than the first-order kinetics. Figure 6 summarizes second-order plots of the reaction at several temperatures.

The second-order kinetics to the Ti complex are consistent with the reaction pathway in Scheme 3 involving disproportionation of **1a** prior to the thiolato ligand transfer from Ti to Pt. Initial disproportionation of **1a** (i) gives **2a**, which reacts with the Pt complex to afford PtMe(SPh)(cod) and to regenerate **1a** (ii). Direct ligand transfer from **1a** to the Pt complex (iii), even if it exists, seems to occur at a much slower reaction rate than the stepwise reactions (i) and (ii) since the total ligand exchange reaction obeys the second-order kinetics. Table 3 summarizes the observed second-order rate constants, $k_{\mathrm{obsd}}$, obtained under various reaction conditions. If reaction (ii) in Scheme 3 would take place much more rapidly than reaction (i), the kinetic formulae should be expressed by a simple second-order kinetics to the Ti complex in Eq. 4, but with $k_{\mathrm{obsd}}$ independent of the initial concentration of the Pt complexes. The observed rate constants, however, vary depending on the concentration of [PtCl(Me)(cod)]$_0$ or the ratio between [PtCl(Me)(cod)]$_0$ and [**1a**]$_0$ even at a constant temperature. Figure 7 plots the reciprocal of the observed rate constants versus [**1a**]$_0$/[PtCl(Me)(cod)]$_0$. A linear relationship is observed in a small [**1a**]$_0$/[PtCl(Me)-(cod)]$_0$ region, which is consistent with the reaction pathway involving disproportionation of **1a** and ensuing reaction of **2a** with the Pt complex.

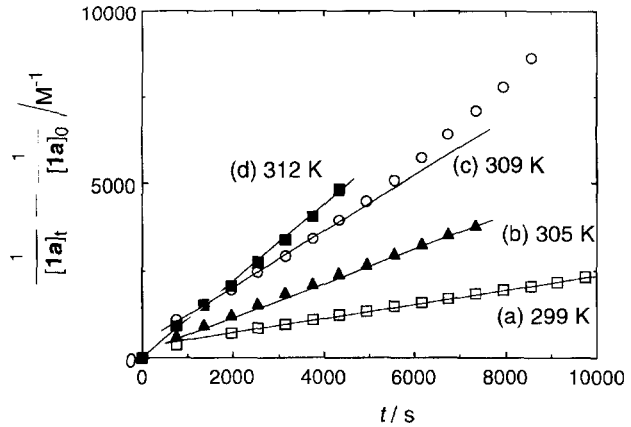


Fig. 6. Second-order plots of the reaction of **1a** with excess PtCl(Me)(cod) obtained from change in the absorption at 500 nm. [**1a**]$_0$ and [**1a**]$_t$ denote concentration of **1a** at the beginning of the reaction and after t seconds, respectively. Reaction conditions are shown in Table 3 (Runs 4, 13, 20, and 24).

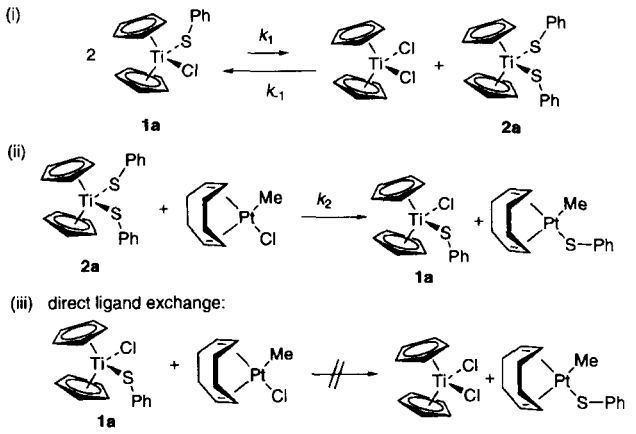


Scheme 3.

Table 3. Observed Second-Order Rate Constants $k_{\mathrm{obsd}}$ of the Reaction of **1a** with PtCl(Me)(cod)[a)]

| Run | [**1a**]$_0$ | [PtCl(Me)(cod)]$_0$ | [**1a**]$_0$ | $T$ | $k_{\mathrm{obsd}}$ |
|---|---|---|---|---|---|
| | mM | mM | [PtCl(Me)(cod)]$_0$ | K | $M^{-1}\,s^{-1}$ |
| 1 | 0.427 | 3.02 | 0.141 | 298.6 | 0.061 |
| 2 | 0.349 | 4.88 | 0.072 | 298.6 | 0.071 |
| 3 | 0.328 | 8.16 | 0.040 | 298.6 | 0.101 |
| 4 | 0.457 | 15.9 | 0.029 | 298.6 | 0.212 |
| 5 | 0.259 | 12.4 | 0.021 | 298.6 | 0.235 |
| 6 | 0.231 | 12.8 | 0.018 | 298.6 | 0.363 |
| 7 | 0.236 | 17.2 | 0.014 | 298.6 | 0.463 |
| 8 | 0.269 | 31.9 | 0.0084 | 298.6 | 0.823 |
| 9 | 0.205 | 20.0 | 0.0010 | 298.6 | 0.883 |
| 10 | 0.589 | 5.17 | 0.114 | 304.6 | 0.157 |
| 11 | 0.348 | 5.21 | 0.067 | 304.6 | 0.182 |
| 12 | 0.396 | 6.92 | 0.057 | 304.6 | 0.190 |
| 13 | 0.310 | 14.8 | 0.021 | 304.6 | 0.482 |
| 14 | 0.293 | 20.5 | 0.014 | 304.6 | 0.612 |
| 15 | 0.307 | 11.8 | 0.026 | 306.6 | 0.231 |
| 16 | 0.383 | 15.3 | 0.025 | 306.6 | 0.291 |
| 17 | 0.226 | 20.1 | 0.011 | 306.6 | 0.838 |
| 18 | 0.279 | 40.2 | 0.0069 | 306.6 | 1.26 |
| 19 | 0.293 | 7.45 | 0.039 | 309.1 | 0.539 |
| 20 | 0.286 | 11.6 | 0.025 | 309.1 | 0.950 |
| 21 | 0.314 | 14.9 | 0.021 | 309.1 | 0.922 |
| 22 | 0.300 | 19.9 | 0.015 | 309.1 | 1.28 |
| 23 | 0.363 | 13.5 | 0.027 | 312.1 | 0.919 |
| 24 | 0.234 | 9.23 | 0.025 | 312.1 | 1.07 |
| 25 | 0.247 | 12.5 | 0.020 | 312.1 | 1.18 |
| 26 | 0.205 | 21.0 | 0.0098 | 312.1 | 2.51 |

a) See Experimental for the detailed reaction procedure.

These results contrast with the previously reported reaction of $Cp_2TiCl(SEt)$, generated in situ, with $PtCl_2(cod)$ in THF, which obeys the first-order kinetics with respect to both the Ti and Pt complexes and involves direct intermolecular

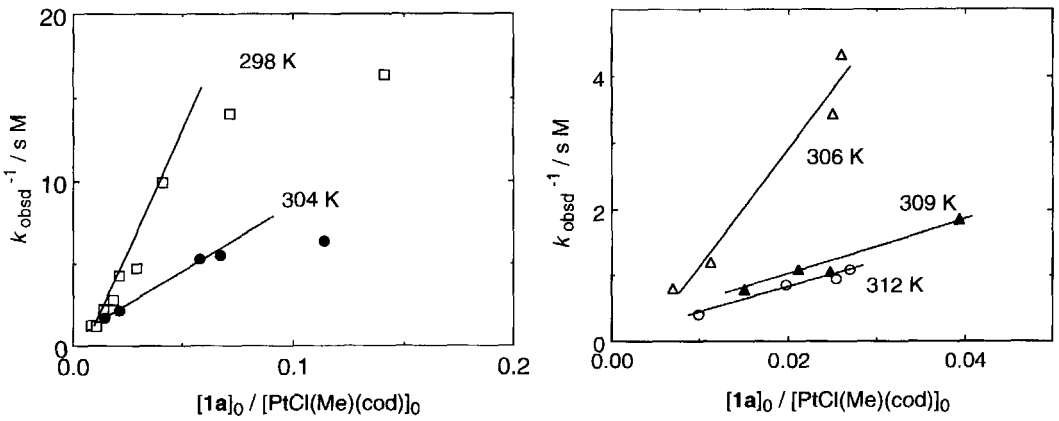


Fig. 7. Plots of reciprocal of the observed rate constants of reaction (3) based on the second-order kinetics to [**1a**].

ligand exchange between the complexes. The thiolato ligand of **1a** is not reactive enough to undergo transfer to the Pt complex, while **2a** with a more highly nucleophilic thiolato ligand could react with PtCl(Me)(cod). This difference in reactivity between the thiolato ligands of **1a** and **2a** which are in equilibrium in THF through reversible disproportionation and conproportionation has enabled the thiolato ligand transfer via the pathway shown in (i) and (ii) in Scheme 3.

**Kinetics of the Reaction of 2a.** In order to obtain a more detailed insight of the reaction of **2a** with PtCl(Me)(cod) giving **1a**, a kinetic study of the reaction was conducted. The change in the absorption spectrum at the initial period of the reaction shows conversion of **2a** into **1a**, as shown in Fig. 5a. Although peaks due to **2a** (540 nm, $\varepsilon = 6000$) and **1a** (500 nm, $\varepsilon = 3500$) markedly overlap with each other, the molar ratios of **1a** to **2a** during the reaction can be obtained by comparing the absorption intensities at 540 and 500 nm with the spectra of solutions containing **1a** and **2a** at several molar ratios. Figure 8 plots the time-dependent decrease in concentration of **2a** in the reaction of it with excess PtCl(Me)(cod). The linear first-order plot of the reaction suggests first-order kinetics to [**2a**]. The reaction is presumed to obey first-order kinetics also to [PtCl(Me)(cod)] although the relationship between observed first-order rate constants and [PtCl(Me)(cod)] was not determined due to insufficient precision of the rate constants arising from the close positions of the peaks due to **1a** and **2a**.

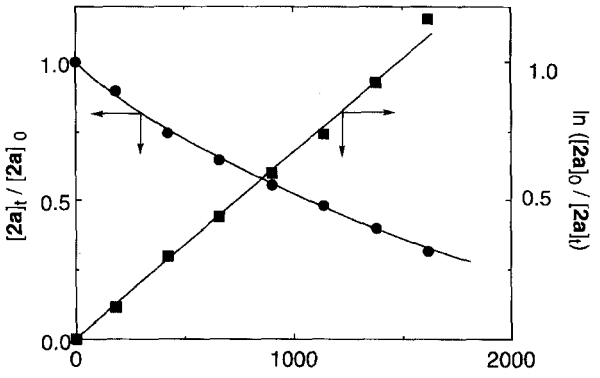


Fig. 8. Time-yield curve and first-order plots of reaction of **2a** with excess PtCl(Me)(cod). The marks ● and ■ denote [**2a**]$_t$/[**2a**]$_0$ and ln ([**2a**]$_0$/[**2a**]$_t$), respectively. Conditions: at 34.0 °C with [**2a**]$_0$ = 0.146 mM and [PtCl(Me)(cod)]$_0$ = 14.3 mM.

Thus, phenylthiolato ligand transfer from Ti to Pt accompanied by Cl ligand transfer from Pt to Ti takes place preferentially via the reaction of **2a** with PtCl(Me)(cod). An intermolecular ligand exchange between **1a** and PtCl(Me)(cod) is not responsible for the formation of the thiolatoplatinum complex **3a**. The ligand exchange between **2a** and the Pt complex seems to occur via an associative pathway involving a Ti–Pt heterobimetallic intermediate,[11–22] similar to the reaction of $Cp_2Ti(SR)_2$ and $PtCl_2(cod)$.[5]

In summary, the present study has established the mechanism of the thiolato ligand transfer from $Cp_2Ti(X)(SAr)$ (X = Cl, SAr) to PtCl(Me)(cod). The methyl ligand bonded to the Pt center behaves as a spectator ligand throughout the reaction. Inertness of the methyl–Pt bond toward the reaction can be ascribed to a high degree of covalent character of the bond which prevents ionic dissociation of the methyl ligand. Rapid and reversible disproportionation of $Cp_2TiCl(SAr)$ type complexes to afford $Cp_2Ti(SAr)_2$ plays an important role in the completion of the reaction. The resulting methyl(thiolato)platinum complexes having a labile cod ligand are of use as precursors of various organoplatinum complexes.

## Experimental

**General Considerations, Materials, and Measurement.** All the manipulations of the complexes were carried out under nitrogen or argon using standard Schlenk technique. The solvents were dried by the usual method, distilled, and stored under nitrogen. Complexes $Cp_2Ti(SPh)_2$, $Cp_2Ti(SC_6H_4Me\text{-}p)_2$, $Cp_2Ti(SC_6H_4Cl\text{-}p)_2$, $Cp_2Ti(SC_6H_4OMe\text{-}p)_2$, $Cp_2Ti(SC_{10}H_7)_2$, and PtCl(Me)(cod), were prepared according to the literature.[23–28] NMR spectra were recorded on a JEOL EX-400 spectrometer. Absorption spectra were obtained with a Hitachi 200-20 spectrophotometer equipped with a thermostatted control by water-jacket. Elemental analyses were carried out with a Yanaco MT-5 CHN autocorder.

**Preparation of 1a.** A mixture of $Cp_2TiCl_2$ (530 mg, 2.1 mmol) and NaSPh (280 mg, 2.1 mmol) was dissolved in THF (15 $cm^3$) at room temperature. Stirring the solution for 12 h at room temperature caused the change in color from orange to red-purple and the deposition of NaCl. Removal of the insoluble solid by filtration

Table 4. Crystallographic Data and Details of Refinement of **1a** and **3a**

| | **1a** | **3a** |
|---|---|---|
| Formula | $C_{16}H_{15}ClSTi$ | $C_{15}H_{20}SPt$ |
| M | 322.71 | 427.47 |
| Crystal system | Orthorhombic | Triclinic |
| Space group | $P2_12_12_1$ (No. 19) | $P\bar{1}$ (No. 2) |
| $a$/Å | 10.961(6) | 8.278(5) |
| $b$/ Å | 13.005(4) | 13.331(5) |
| $c$/ Å | 10.566(5) | 7.197(4) |
| $\alpha$/° | | 102.16(5) |
| $\beta$/° | | 113.09(4) |
| $\gamma$/° | | 94.65(5) |
| $V$/Å$^3$ | 1506(1) | 702.3(7) |
| $Z$ | 4 | 2 |
| $\mu$/mm$^{-1}$ | 0.867 | 10.08 |
| Unique reflections | 1994 | 3233 |
| Used reflections[a)] | 665 | 2500 |
| No. of variables[b)] | 122 | 154 |
| $R$ ($R_w$)[c)] | 0.065 (0.046) | 0.043 (0.034) |

a) $F_o > 2\sigma(F_o)$ for **1a** and $F_o > 3\sigma(F_o)$ for **3a**. b) Cyclopentadienyl carbon atoms are refined isotropically. c) Weighting scheme, $[\{\sigma(F_o)\}^2]^{-1}$.

and ensuing evaporation of the filtrate to dryness gave a red-purple solid (352 mg). Repeated recrystallization of the product from $CH_2Cl_2$–$Et_2O$ afforded **1a** as red-purple crystals (125 mg, 18%). Anal. Calcd for $C_{16}H_{15}ClSTi$: C, 57.99; H, 4.87; Cl, 11.41; S: 10.32%. Found: C, 58.53; H, 4.49; Cl, 11.69; S: 9.02%. $^1$H NMR (benzene-$d_6$) $\delta$ = 5.79 (s, 10H, $C_5H_5$), 6.95 (t, 1H, para, $J$ = 7 Hz), 7.12 (d, 2H, meta), 7.73 (d, 2H, ortho, $J$ = 9 Hz). Precise $J$(HH) values of the meta hydrogen signals were not determined due to severe overlap with the solvent signal.

Dissolution of **1a** in THF-$d_8$ caused its reversible disproportionation into **2a** and $Cp_2TiCl_2$. Equilibrium constants of the disproportionation were determined based on the $^1$H NMR peak area ratio of the cyclopentadienyl ligand hydrogens as follows: $K_{eq} = [Cp_2TiCl_2][\mathbf{2a}]/[\mathbf{1a}]^2 = 0.0304$ (300.3 K), 0.0342 (307.9 K), 0.0380 (312.9 K), 0.0399 (317.8 K), 0.0438 (322.9 K).

**Reactions of PtCl(Me)(cod) with 2a—2e.** To a mixture of PtCl(Me)(cod) (90 mg, 0.25 mmol) and **2a** (101 mg, 0.25 mmol) in a Schlenk flask was added THF (6 cm$^3$) at room temperature. The purple reaction mixture gradually became red-purple. After evaporation of the solvent to 3 cm$^3$, acetone (3 cm$^3$) was added to cause precipitation of a solid. The resulting solid was collected by filtration and washed with acetone (2 cm$^3$) and then with hexane (5 cm$^3$) and dried in vacuo to give **3a** as a colorless solid (81 mg, 75%). Evaporation of the filtrate to dryness led to a mixture of **1a**, **2a**, $Cp_2TiCl_2$ and $[(Cp_2Ti)_2O]$ (69 mg).

Reactions of PtCl(Me)(cod) with **2b**—**2e** were carried out analogously. The $^1$H NMR data (benzene-$d_6$) of **1b**—**1e** (**1b**: Ar = $C_6H_4Me$-*p*, **1c**: Ar = $C_6H_4OMe$-*p*, **1d**: Ar = $C_6H_4Cl$-*p*, **1e**: Ar = $C_{10}H_7$) observed in a mixture with the Ti complexes are as follows. Data for **1b**: $\delta$ = 1.93 (s, 3H, $CH_3$), 5.82 (s, 10H, $C_5H_5$), 6.76 (d, 2H, $C_6H_4$, $J$ = 8 Hz), 7.64 (d, 2H, $C_6H_4$, $J$ = 8 Hz). Data for **1c**: $\delta$ = 3.26 (s, 3H, $OCH_3$), 5.82 (s, 10H, $C_5H_5$), 6.76 (d, 2H, $C_6H_4$, $J$ = 8 Hz), 7.63 (d, 2H, $C_6H_4$, $J$ = 9 Hz). Data for **1d**: $\delta$ = 5.73 (s, 10H, $C_5H_5$), 7.05 (d, 2H, $C_6H_4$, $J$ = 8 Hz), 7.44 (d, 2H, $C_6H_4$, $J$ = 8 Hz). Data for **1e**: $\delta$ = 5.81 (s, 10H, $C_5H_5$), 7.04—8.27 (m, 7H, $\alpha$-$C_{10}H_7$).

**Kinetic Measurement.** A Schlenk flask attached to an optical cell was filled with argon. PtCl(Me)(cod) (21 mg, 0.060 mmol) was placed in the optical cell part. A THF (3.7 cm$^3$) solution of **1a** (0.31 mM), prepared by the trap-to-trap distillation of the solvent dried over Na-benzophenone immediately before use, was transferred to the flask with a cannula. After the system was sealed, the flask was immersed in a thermostatted bath for 0.5 h. Then, the solution was transferred to the optical cell to dissolve the Pt complex in it. The time-yield curve of the reaction was recorded by periodic measurements of the spectrum or by following the intensity of absorption at a fixed wavelength. The temperature of the solution was directly measured after completion of the reaction.

**Crystal Structure Determination.** Crystals of **1a** and **3a** suitable for X-ray diffraction study were obtained by recrystallization from $CH_2Cl_2$–hexane and mounted in glass capillary tubes under argon. Intensities were collected for Lorentz and polarization effects on a Rigaku AFC-5R automated four-cycle diffractometer by using Mo $K\alpha$ radiation ($\lambda$ = 0.71069 Å) and $\omega$–2$\theta$ scan method, and an empirical absorption correction ($\Psi$ scan) was applied. Calculations were carried out by using a program package TEXSAN on a DEC Micro VAX-II computer. Atomic scattering factors were obtained from the literature.[29] A full matrix least-squares refinement was used for non-hydrogen atoms with anisotoropic thermal parameters. Hydrogen atoms were located by assuming the ideal geometry and these locations were included in the structure calculation without further refinement of the parameters. Crystallographic data and details of refinement are summarized in Table 4. All the data of the crystallographic study including $F_o - F_c$ tables are deposited as Document No. 73019 at the Office of the Editor of Bull. Chem. Soc. Jpn. Crystallographic data are deposited also at the CCDC, 12 Union Road, Cambridge CB2 1EZ, UK and copies can be obtained on request, free of charge, by quoting the publication citation and the deposition numbers 139444-139445.

This work was financially supported by a Grant-in-Aid for Scientific Research on Priority Areas "Inter-element Linkage", No. 09239212 from the Ministry of Education, Science, Sports and Culture.

## Appendix

The kinetic expressions of the stepwise reactions (i) and (ii) in Scheme 3 as well as the derivations are summarized below. The rate of the reactions is expressed by the two equations (5) and (6).

$$-\frac{d[\mathbf{1a}]}{dt} = k_1[\mathbf{1a}]^2 - k_{-1}\frac{[\mathbf{1a}]_0 - [\mathbf{1a}]}{2}[\mathbf{2a}] - k_2[\mathbf{2a}][PtCl(Me)(cod)], \quad (5)$$

$$\frac{d[\mathbf{2a}]}{dt} = \frac{1}{2}k_1[\mathbf{1a}]^2 - \frac{1}{2}k_{-1}\frac{[\mathbf{1a}]_0 - [\mathbf{1a}]}{2}[\mathbf{2a}] - k_2[\mathbf{2a}][PtCl(Me)(cod)]. \quad (6)$$

On assuming $\frac{d[\mathbf{2a}]}{dt} = 0$,

$$\frac{1}{2}k_1[\mathbf{1a}]^2 = \left\{\frac{1}{4}k_{-1}([\mathbf{1a}]_0 - [\mathbf{1a}]) + k_2[PtCl(Me)(cod)]\right\}[\mathbf{2a}], \quad (7)$$

$$[\mathbf{2a}] = \frac{2k_1[\mathbf{1a}]^2}{k_{-1}([\mathbf{1a}]_0 - [\mathbf{1a}]) + 4k_2[PtCl(Me)(cod)]}. \quad (8)$$

$$-\frac{d[\mathbf{1a}]}{dt} = k_1[\mathbf{1a}]^2 - \left\{\frac{k_{-1}([\mathbf{1a}]_0 - [\mathbf{1a}])}{2} - k_2[PtCl(Me)(cod)]\right\} \times \frac{2k_1[\mathbf{1a}]^2}{k_{-1}([\mathbf{1a}]_0 - [\mathbf{1a}]) + 4k_2[PtCl(Me)(cod)]}$$
$$= k_1[\mathbf{1a}]^2\left\{1 - \frac{k_{-1}([\mathbf{1a}]_0 - [\mathbf{1a}]) - 2k_2[PtCl(Me)(cod)]}{k_{-1}([\mathbf{1a}]_0 - [\mathbf{1a}]) + 4k_2[PtCl(Me)(cod)]}\right\}$$
$$= k_1[\mathbf{1a}]^2\frac{2k_2[PtCl(Me)(cod)]}{k_{-1}([\mathbf{1a}]_0 - [\mathbf{1a}]) + 4k_2[PtCl(Me)(cod)]}. \quad (9)$$

Consequently

$$-\frac{k_{-1}[\mathbf{1a}]_0 + 4k_2[PtCl(Me)(cod)] - k_{-1}[\mathbf{1a}]}{[\mathbf{1a}]^2}\frac{d[\mathbf{1a}]}{dt} = 2k_1k_2[PtCl(Me)(cod)], \quad (10)$$

$$-\frac{(k_{-1}[\mathbf{1a}]_0 + 4k_2[PtCl(Me)(cod)]) - k_{-1}[\mathbf{1a}]}{[\mathbf{1a}]^2}d[\mathbf{1a}] = 2k_1k_2[PtCl(Me)(cod)]dt, \quad (11)$$

$$\frac{(k_{-1}[\mathbf{1a}]_0 + 4k_2[PtCl(Me)(cod)])}{[\mathbf{1a}]} + k_{-1}\ln[\mathbf{1a}] = 2k_1k_2[PtCl(Me)(cod)]t + C. \ (C: \text{ constant}) \quad (12)$$

The change in $k_{-1}\ln[\mathbf{1a}]$ depending on the decrease of [**1a**] from $[\mathbf{1a}]_0$ to $[\mathbf{1a}]_0$ ($\approx 0$) is much smaller than that in $k_{-1}[\mathbf{1a}]_0/[\mathbf{1a}]$. Thus the second term in the left part of Eq. 12 is dependent on t to a negligible extent and can be regarded as a constant. By introducing $[PtCl(Me)(cod)] = [PtCl(Me)(cod)]_0$ and $[\mathbf{1a}]_t = [\mathbf{1a}]$ at time $t$, one finds

$$\frac{(k_{-1}[\mathbf{1a}]_0 + 4k_2[PtCl(Me)(cod)]_0)}{[\mathbf{1a}]_t} = 2k_1k_2[PtCl(Me)(cod)]_0t + C'. \quad (13)$$

Since $\frac{1}{[\mathbf{1a}]t} - \frac{1}{[\mathbf{1a}]0} = k_{obsd}t$,

$$k_{obsd} = \frac{2k_1k_2[PtCl(Me)(cod)]_0}{k_{-1}[\mathbf{1a}]_0 + 4k_2[PtCl(Me)(cod)]_0},$$
$$\frac{1}{k_{obsd}} = \frac{k_{-1}}{2k_1k_2}\frac{[\mathbf{1a}]_0}{[PtCl(Me)(cod)]_0} - \frac{2}{k_1}. \quad (14)$$

Thus, a linear relationship between $1/k_{obsd}$ and $[\mathbf{1a}]_0/[PtCl(Me)(cod)]_0$ shown in Fig. 7 is derived.

## References


1 C. M. Bolinger and T. B. Rauchfuss, *Inorg. Chem.*, **21**, 3947 (1982).

2 A. Shaver, S. Morris, R. Turrin, and V. W. Day, *Inorg. Chem.*, **29**, 3622 (1990).

3 T. A. Wark and D. W. Stephan, *Can. J. Chem.*, **68**, 565 (1990).

4 A. Yamaguchi, T. Fujita, M. Kajitani, T. Akiyama, and A. Sugimori, "65th Annual Meeting of Chemical Society of Japan," 1993, Abstr., No. 2P08.

5 K. Osakada, Y. Kawaguchi, and T. Yamamoto, *Organometallics*, **14**, 4542 (1995).

6 C. K. Johnson, "ORTEP, Report ORNL-5138," Oak Ridge National Laboratory, Oak Ridge, TN (1976).

7 E. G. Müller, S. F. Watkins, and L. F. Dahl, *J. Organomet. Chem.*, **111**, 73 (1976).

8 T. T. Nadasdi and D. W. Stephan, *Organometallics*, **11**, 116 (1992).

9 P. C. Bulman Page, S. S. Klair, M. P. Brown, M. M. Harding, C. S. Smith, S. J. Maginn, and S. Muley, *Tetrahedron Lett.*, **29**, 4477 (1988).

10 C. E. Briant, C. J. Gardner, T. S. Andy Hor, N. D. Howells, and D. M. P. Mingos, *J. Chem. Soc., Dalton Trans.*, **1984**, 2645.

11 T. S. Cameron, C. K. Prout, G. V. Rees, M. L. H. Green, K. K. Joshi, G. R. Davies, B. T. Kilbourn, P. S. Braterman, and V. A. Wilson, *J. Chem. Soc., Chem. Commun.*, **1971**, 14.

12 M. Sato and T. Yoshida, *J. Organomet. Chem.*, **94**, 403 (1975).

13 H. Werner, B. Ulrich, U. Schubert, P. Hofmann, and B. Zimmer-Gasser, *J. Organomet. Chem.*, **297**, 27 (1985).

14 C. J. Ruffing and T. B. Rauchfuss, *Organometallics*, **4**, 524 (1985).

15 W. E. Douglas and M. L. H. Green, *J. Chem. Soc., Dalton Trans.*, **1972**, 1796.

16 M. Y. Darensbourg, M. Pala, S. A. Houliston, K. P. Kidwell, D. Spencer, S. S. Chojnacki, and J. H. Reibenspies, *Inorg. Chem.*, **31**, 1487 (1992).

17 G. S. White and T. W. Stephan, *Organometallics*, **6**, 2169 (1987).

18 T. A. Wark and D. W. Stephan, *Inorg. Chem.*, **26**, 363 (1987).

19 T. A. Wark and D. W. Stephan, *Organometallics*, **8**, 2836 (1989).

20 R. Rousseau and D. W. Stephan, *Organometallics*, **10**, 3399 (1991).

21 T. A. Wark and D. W. Stephan, *Inorg. Chem.*, **29**, 1731 (1990).

22 T. T. Nadasdi and D. W. Stephan, *Inorg. Chem.*, **33**, 1532 (1994).

23 H. Köpf and M. Schmidt, *J. Organomet. Chem.*, **4**, 426 (1965).

24 H. Köpf and M. Schmidt, *Z. Anorg. Allg. Chem.*, **340**, 139 (1965).

25 T. Klapötke and H. Köpf, *Inorg. Chim. Acta*, **133**, 115 (1987).

26 R. S. P. Coutts, J. R. Surtees, J. M. Swan, and P. C. Wailes, *Aust. J. Chem.*, **19**, 1377 (1966).

27 M. A. Chaudhari and F. G. A. Stone, *J. Chem. Soc. A*, **1966**, 838.

28 S. A. Giddings, *Inorg. Chem.*, **6**, 849 (1967).

29 "International Tables for X-Ray Crystallography," Kynoch, Birmingham, England (1974).